

Polyethylene under tensile load: strain energy storage and breaking of linear and knotted alkanes probed by first-principles molecular dynamics calculations

A. Marco Saitta* and Michael L. Klein

Center for Molecular Modeling, Dept. of Chemistry, University of Pennsylvania, Philadelphia, PA 19104-6202

(May 6, 2018)

The mechanical resistance of a polyethylene strand subject to tension and the way its properties are affected by the presence of a knot is studied using first-principles molecular dynamics calculations. The distribution of strain energy for the knotted chains has a well-defined shape that is very different from the one found in the linear case. The presence of a knot significantly weakens the chain in which it is tied. Chain rupture invariably occurs just outside the entrance to the knot, as is the case for a macroscopic rope.

I. INTRODUCTION

Structural isomerism is a well-studied phenomenon in chemistry, but it is also possible to construct isomers of molecules that differ not in their connectivity, but in their topology [1–3]. These topological isomers exhibit different optical rotary power. Examples of topologically complicated structures are knots, for which the simplest is the “trefoil”. A trefoil is constructed from one chain that forms a single, self-threaded loop [4,5]. Technically, the ends of the chain must be connected for this structure to be a knot [6]. DNA fragments, for example, have been observed to form knots similar to the trefoil as well as more complicated ones [7]. Interpenetrating entangled polymers also form knots. Statistical arguments based on self-avoiding random walks, Hamilton cycles, and so on, have demonstrated conclusively that the chain length is the crucial factor governing the probability of knot formation [8,9]. As the chain length increases, this probability goes to one exponentially [10].

The self-entanglement of polymer chains has profound effects on the physical properties of the bulk material, such as its crystallization behavior, elasticity, and rheology. For example, the transfer of a knot from a polymer in the melt state to that in the crystalline/glassy state has been studied [11]. Crystallization of polymers is inhibited by the presence of knots and the freezing tends to remove them. On the other hand, quenching the melt to a glass tightens and stabilizes existing knots. The structure and stability of knots in polymers has been a subject of extensive study [12–15]. We recently reported a first-principles molecular dynamics study of a trefoil knot in a polyethylene strand, which revealed a surprising similarity in behavior between macroscopic and microscopic knotted strands under tensile stress [16]. In the present work, we focus on the storage of strain energy in a polymer. In particular, we will describe how strain distributions differ between linear and knotted polymer chains. Further, this work demonstrates that an efficient combination of classical [17] and density-functional based first-principles [18] molecular dynamics (MD) can be a very

useful tool in the description of physical as well as chemical properties of polymers with and without topological defects.

The essential details of the calculations are provided in the following section. The results for the linear polyethylene-like (alkane) molecules are reported in Section III, while classical and first-principles simulations on the knotted strands are presented in Section IV. We discuss our findings in Section V.

II. COMPUTATIONAL METHOD

The first principles calculations were performed using the Car-Parrinello (CP) method [18], which combines MD and density-functional theory (DFT). DFT is known to provide an accurate and reliable description of carbon- and hydrocarbon-based systems [19]. We adopted Becke and Lee-Yang-Parr (BLYP) [20] gradient corrections to describe the exchange and correlation functionals, respectively. The electron-ion interaction was described by pseudopotentials in the Martins-Troullier [21] form. The plane-wave basis set had a cutoff of 60 Ry, with a Γ -point integration in the Brillouin zone. Electron spin was explicitly taken into account [22], to obtain more reliable values of the dissociation energies. We described the isolated molecules with periodic boundary conditions and supercells that were large enough to avoid any significant interaction with periodic images. The same, large, tetragonal supercell ($12 \text{ \AA} \times 12 \text{ \AA} \times 20 \text{ \AA}$) was used in both the linear and knotted cases. While these dimensions may be oversized for the linear molecules, this approach afforded us consistent and comparable results.

Classical MD simulations were carried out according to the united atom (UA) scheme [23], in which every methylene ($-CH_2-$) or methyl ($-CH_3$) group is considered a “pseudoatom”. The potential of interaction included harmonic bond-stretching, harmonic bond-bending, a torsional field, and a Lennard-Jones interaction between non-bonded atoms. We fitted the stretching and bending interaction constants of the model to *ad hoc* CP calcula-

tions on small alkanes.

In both classical and first-principles MD simulations, external tensile stress was mimicked by constraining the chain end-to-end distance L to a fixed value. The system was evolved dynamically at room temperature before being annealed in order to find the (constrained) minimum.

III. LINEAR ALKANES

All the results reported in this section refer to CPMD simulations. As a first step, we studied a decane molecule ($C_{10}H_{22}$), which can be taken as representative of longer linear alkanes and, by extrapolation, of polyethylene. The equilibrium structural parameters, reported in Table 1, are in excellent agreement (within 1%) with other DFT results and with experimental data [24,25] for hydrocarbons and/or crystalline polyethylene (PE).

The molecule was stretched in a series of steps. Additional external load was applied to the system by successively increasing L . To do so, the nuclear coordinates were all scaled uniformly along the molecular z axis. In the first stages of tensile loading, the geometry of the system was optimized by minimizing the forces acting on atoms, but no dynamics was used. Quite unexpectedly, the strain did not distribute uniformly along the chain, but tended to concentrate equally on the two extremal bonds, where the force originating from the constraint was actually applied. This behavior can be clearly observed by comparing the terminal \widehat{CCC} bond angles and $C-C$ bond lengths with the average values calculated for atoms in the interior of the chain. These results are reported in panels **a** and **b** of Fig. 1 as a function of the distance L . For deformations ΔL larger than 10% of the equilibrium length L_0 , we followed the procedure, described in the previous section, of letting the molecule evolve dynamically at room temperature, and then cooling it down with a simulated annealing technique. The global constrained minimum of the system, after the CPMD evolution, was found by geometry optimization of the structure. The linear n -decane does not break for distortions up to $\Delta L \sim 18.0\%$.

	$C_{10}H_{22}$ (BLYP)	$C_{10}H_{22}$ (BP)	Cryst. PE (BP)	Cryst. PE (exp.)
d_{CC}	1.54	1.53	1.54	1.55(2)
d_{CH}	1.10	1.10	1.11	1.09(1)
α_{CCC}	114	113	114	111(3)
α_{HCH}	107	108	106	108(2)

TABLE I. Equilibrium structural parameters of n -decane as determined in the present work (DFT-BLYP) or using a Becke-Perdew (DFT-BP) functional for the exchange and correlation (23), compared to theoretical (DFT-BP) and experimental results for crystalline polyethylene (PE) (23,24).

The distribution of strain energy of the system was estimated by adopting the UA model [23] to analyze the configurations provided by the first-principles calculations. In the present case, contributions to the total strain energy originating from the torsional potential and the long-range non-bonded interactions are negligible. Bond stretching and bending largely dominate in the storage of tensile load in linear molecules. The system can sustain about 16.2 kcal/mol per $C-C$ bond before rupture (Fig. 1, panel **c**).

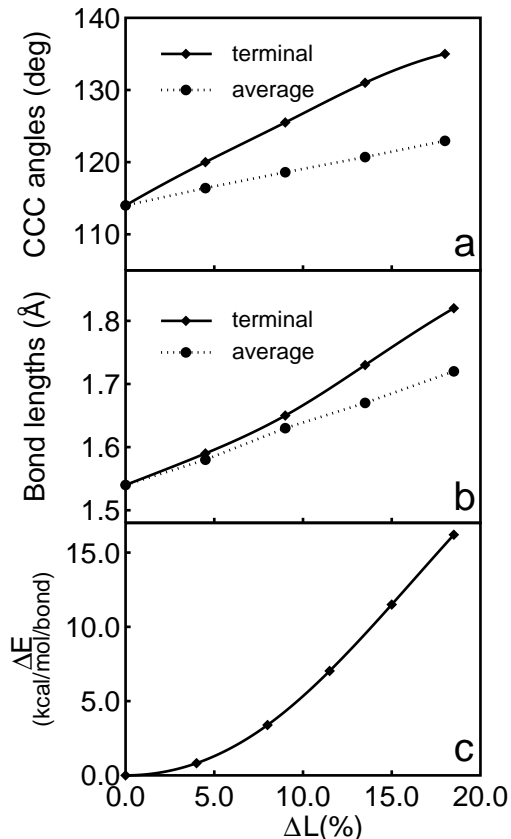


FIG. 1. Analysis of the strain distribution along the n -decane molecule as function of the linear deformation. In panel **a** shown is the bond angle (degrees) of the terminal carbons (diamonds, solid line), and the average *other* $C-C-C$ bond angles (circles, dotted line). In panel **b** we report the $C-C$ bond-length (\AA) distribution accordingly. In panel **c** the average strain energy (kcal/mol) per $C-C$ bond is displayed.

The analysis of the strain energy distribution along the chain for $L = 1.18 L_0$, shown in Fig. 2, confirmed the results previously discussed, *i.e.*, the stress was not uniform along the molecule. Instead, it was mostly concentrated on the two extremal bonds, which store 20-25 kcal/mol of the energy associated with the distortions from the ideal geometry. All the other “central” bonds sustain a lower stress, whose average energy is about 12 kcal/mol.

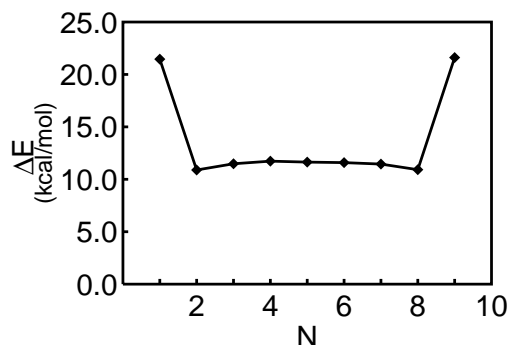


FIG. 2. Strain energy distribution along the $C-C$ bonds of the n -decane molecule for a deformation $\Delta L = 18\%$, estimated by making use of the UA model (see text). The stress is seen to concentrate most on the extremal bonds, while being almost constant along the others.

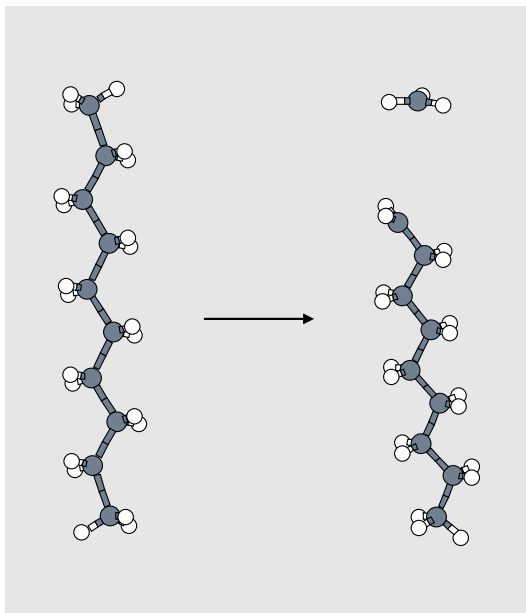


FIG. 3. A strained ($L = 1.18 L_0$) n -decane molecule before (left) and after (right) bond breakage. Carbons are displayed in dark gray and hydrogens in white. The $sp^3 \rightarrow sp^2$ change of the hybridization status of the atoms involved is detectable from the coplanarity of the two carbons with their bonds.

The qualitative features of the strain energy distribution were essentially the same for any value of length deformation, ΔL . The bonds closest to the two extremal ones typically were about 6% energetically less strained than the average of the central bonds. Thus, from the third atom on, the system can be considered to be “bulk”, and the strain practically constant. Additional calculations performed on a linear $C_{21}H_{44}$ molecule indicate that the shape of the strain energy distribution reported in Fig. 2 for $C_{10}H_{22}$ is unaffected by the size of the system. The amount of strain energy on the extremal and

the “bulk” bonds are within the errors of the values obtained for the shorter alkane.

As foreshadowed by the classical strain energy distribution, the CPMD simulation results demonstrated that, for larger elongations, the alkane molecule actually breaks at one of the extremal bonds. As shown in Fig. 3, the $C_9H_{19}\cdot$ radical contracts very quickly after the break. While large deviations from equilibrium bond lengths were found throughout the simulations, the true marker for bond dissociation was the change in hybridization ($sp^3 \rightarrow sp^2$) for the previously bonded carbon atoms. Indeed, as shown in the right side of Fig. 3, the three bonds about those carbon atoms become coplanar after the break. The length of the bond formed between the last carbon atom of the $C_9H_{19}\cdot$ radical and its closest neighbor decreases as well, oscillating around the typical $C_{(sp^3)}$ -like value, *ca.* 1.49 Å. The experimental enthalpy of dissociation of a methyl group from smaller n -alkanes is *ca.* 86 kcal/mol. Our theoretical dissociation energy of 83 kcal/mol, calculated as the energy difference between the optimized $C_{10}H_{22}$ molecule and the optimized radicals, gives a very good quantitative description of the dissociation phenomenon.

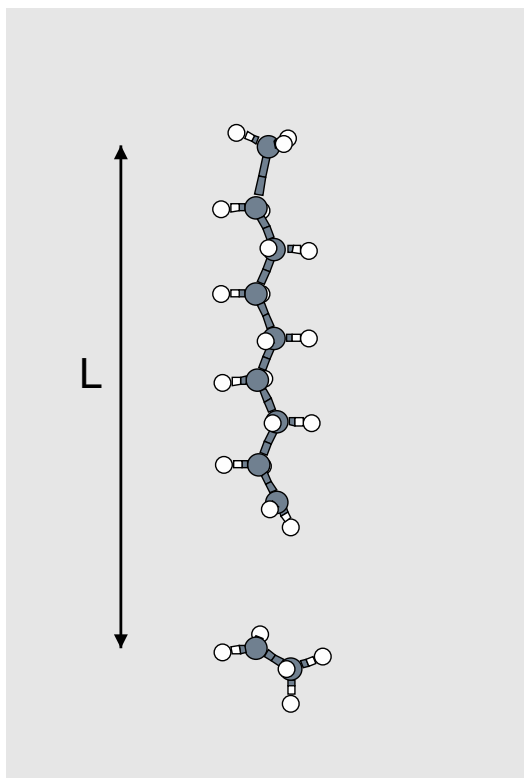


FIG. 4. The n -undecane molecule after bond breakage. As displayed, the constraint on the distance L is applied between C_1 and C_{10} . The resulting sp^2 hybridization of C_9 and C_{10} is clearly observable.

The finding that a linear alkane subject to tensile stress breaks where the external force is applied was

checked by performing analogous simulations with a n -undecane molecule ($C_{11}H_{24}$). In this case, however, the constrained distance L was not the end-to-end length of the chain, but still the C_1 - C_{10} distance. Indeed, this system behaved very similarly. As was observed for the n -decane molecule, the chain once again ruptured where the constraint was applied. In contrast to the previous case, however, the simulation consistently formed an ethyl radical ($C_{11}H_{24} \rightarrow C_9H_{19}\cdot + C_2H_5\cdot$) (see Fig. 4). The present DFT value for the dissociation energy is 81 kcal/mol, which is again in excellent agreement with the experimental dissociation enthalpy of an ethyl group which is about 82 kcal/mol. We note here that similar calculations that do not take into account spin variables give the same qualitative results, but the corresponding dissociation energies (102 and 94 kcal/mol, respectively) are overestimated by 10-15 %.

IV. KNOTTED MOLECULES

A. Classical MD calculations

The study of a knotted polymer requires a non-trivial procedure to set up the starting nuclear coordinates for a trefoil. Ideally, the behavior of the system should not be biased in any way by a specific strain distribution due to a particular choice of the initial configuration. Further, the computational demands of CPMD calculations prohibit the study of loose knots because of the large system size required. Moreover, the initial stress must be close to, yet below, the breaking threshold to allow the rupture to occur within the typical time scales (< 10 ps) of CPMD. With these constraints in mind, we first performed classical MD simulations with the UA model.

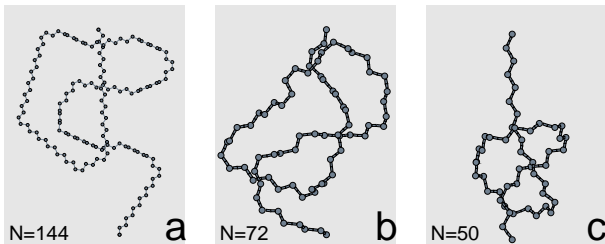


FIG. 5. Initial configurations of the chains containing $N=144$ (a), 72 (b), and 50 (c) pseudoatoms, respectively.

We chose as the initial system a chain of 144 pseudoatoms, and generated the trefoil knot by adding an appropriate set of *gauche* defects to a linear polymer (Fig. 5, panel a). As we mentioned in section II, we performed the MD calculations by anchoring the end atoms of the polymer at a fixed separation distance L , which was then successively increased from one set of simulations to the next. As the knot was tightened, fewer atoms were di-

rectly involved in the formation of the knot and hence they could be removed (Fig. 5, panels b and c).

Longer simulations were performed when the size of the molecule was reduced to $N = 50$ pseudoatoms. First, the system was kept at room temperature for at least 200 ps before cooling it down, with a slow annealing (about 50 ps), to $T = 0$ K. The strain-energy distribution of each chain at the constrained (knotted) minimum energy configurations was systematically determined for each value of the external load. The results obtained from the CP calculations on the linear hydrocarbons suggest that such systems can sustain a strain-energy per bond in the range of 15-30 kcal/mol before rupture. It is thus noteworthy that the per bond strain energy for $N = 50$ chain is negligible on this “relevant” energy scale (Fig. 6), even though the shape of the trefoil is very well defined (Fig. 5, panel c).

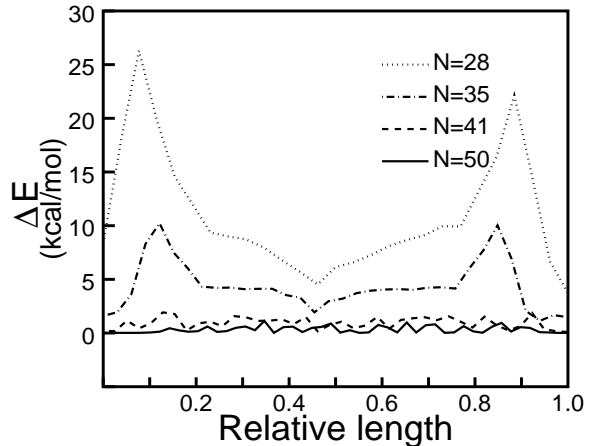


FIG. 6. Classical strain energy distribution along the chains as obtained after room temperature MD evolution and annealing. Shown are results for chains containing $N=50$ (solid line), 41 (dashed line), 35 (dot-dashed line), and 28 (dotted line) pseudoatoms. Polymer lengths (horizontal axis) are scaled in order to facilitate direct comparison among different length molecules.

Fig. 6 shows that decreasing the number of atoms to $N = 41$ does not produce any noticeable effect; when $N = 35$, however, the presence of the knot begins to affect the strain distribution of the system in a significant way [5]. As we will see later, that strain distribution is a general fingerprint of the presence of a trefoil; distortions from ideal geometry tend to concentrate on the entrance and exit points of the knot, while its central portion is much less stressed. By decreasing of the number of pseudoatoms to $N = 28$, the system becomes very close to the “critical” limit. The ideal chain length for our CPMD study thus ranges between 28 and 30 carbon atoms. For both of these values of N , we performed several 500 ps length classical simulations at different tem-

peratures, which were started from varying initial conditions. This was followed by 100 *ps* of slow simulated annealing to obtain a statistically meaningful set of constrained equilibrium configurations for the trefoil under tension. We observed that, for any given length L , deviations in the final configurations obtained from different simulations were so small that the strain energy distribution curves could actually be superimposed on each other with no noticeable difference. The initial configurations for the CP simulations were generated by averaging this set of constrained ground-state positions.

B. CPMD calculations

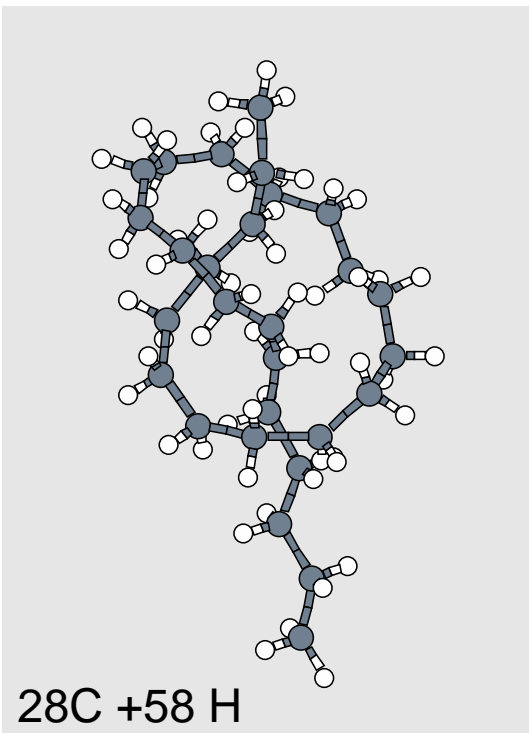


FIG. 7. Sample of initial configuration used in the *ab initio* simulations of the $C_{28}H_{58}$ molecules. The positions of the carbon atoms are obtained from the classical MD simulations, and hydrogens are added to each carbon according to the appropriate tetrahedral symmetry.

The knotted minimum energy configuration obtained from the previous section was decorated with hydrogens atoms according to the ideal tetrahedral symmetry of carbon atoms in alkanes. Structural relaxation showed that this initial guess for the hydrogen positions was very close to those found with minimum energy geometry in the distorted system. In Fig. 7 we show a sample starting configuration of a $C_{28}H_{58}$ *n*-alkane.

CP simulations were carried out with the same technique adopted for the linear alkanes, in which external tensile stress was applied by constraining the end-to-end distance L . Results for the $C_{28}H_{58}$ and $C_{30}H_{62}$

molecules were very similar. Henceforth, unless specified, we will only refer to calculations for the $N = 28$ carbon alkane. Several sets of simulations were carried out for $L = 10.75, 11.50, 12.50, 13.00, 13.50, 13.75$, and 14.00 Å, respectively. For each value of L , the initial positions were optimized (with the constraint) before heating the system to room temperature. We employed smaller timesteps and longer simulations as compared to the linear molecules case. As explained above, this should prevent the initial conditions from biasing the behavior of the system. The sound velocity of polyethylene along the chain direction in the crystal [17] is about 18 km/s and thus an estimate of the time needed for the slowest longitudinal phonon to travel along a 30-atom chain is about 0.25 *ps*; this is the lower bound for the time scale of our calculations. We actually performed CPMD simulations at least 3 or 4 times longer than this value.

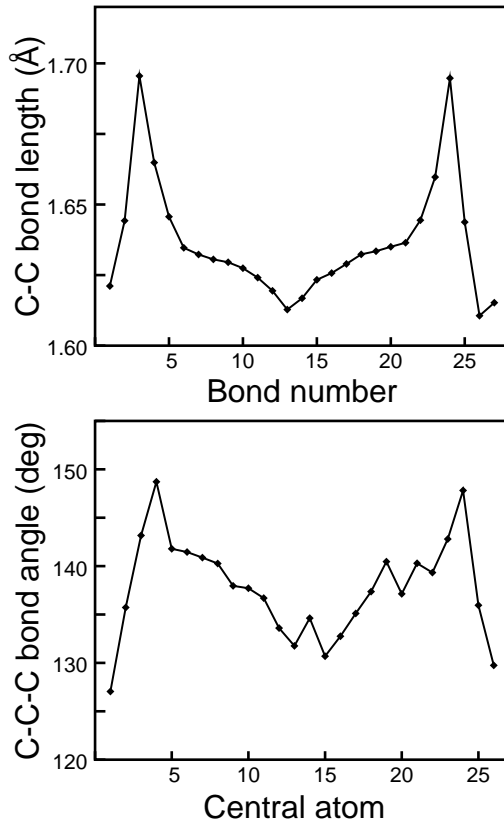


FIG. 8. Distribution of bond lengths and angles in the $C_{28}H_{58}$ alkane at $L = 13.0$ Å. The largest deviations from the equilibrium values occur at the entrance and exit points of the knot.

The optimized *ab initio* structure is typically more favorable by 100-120 kcal/mol as compared to the classical ground-state configuration. The average classical strain energy distributions obtained during finite temperature CPMD runs show a very similar shape to the classical ground-state distributions, but with a larger amount of

strain located on the bonds at the entrance and exit points of the knot, along with a relaxation of the central portion of the knot. This is analogous to the results reported elsewhere [16] and suggests that localized spikes in the strain distribution are necessary to allow global relaxation for the remaining portions of the carbon backbone. In analogy with the linear case, it is interesting to note that the second bond at each end is the least distorted of the whole chain. This bond is neither inside the knot nor the one at which the constraint force is applied.

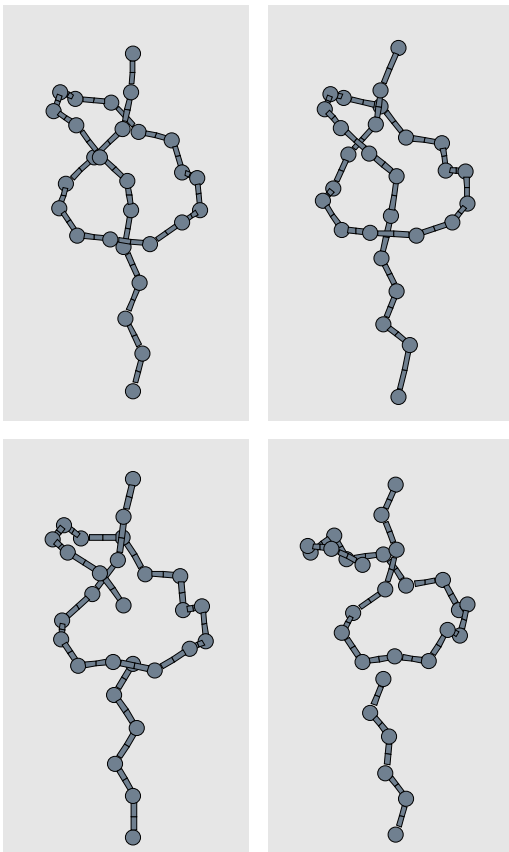


FIG. 9. Snapshots of CP dynamical evolution of the knotted $C_{28}H_{58}$ alkane. For the sake of clarity we only display the carbon backbone. The end-to-end distance in the simulations presently shown is $L = 13.5 \text{ \AA}$, and the temperature is $T = 300 \text{ K}$.

The system does not cross the dissociation barrier at room temperature within the time scale of the simulations for elongations smaller than $L = 13.5 \text{ \AA}$. Larger and larger fluctuations of bond lengths, up to 30 % of the equilibrium values (1.54 \AA), are observed along the dynamical evolution as L increased. This is particularly true for the bonds located at the entrance and exit points of the knot; however, no bonds dissociated. In Fig. 8 we report an example of the $C-C$ bond length and \widehat{CCC} angle distributions along the molecule for $L = 13.0 \text{ \AA}$. The largest deviations from equilibrium values were about 10 % in the lengths and 30 % in the angles; they oc-

curred near the entrance and exit points of the knot. In contrast, the average deviations in the central portion of the knot were *ca.* 5 % and 18 %, respectively.

Our data analysis indicated that monitoring the bond angles about the two atoms forming a bond was a much more effective method to determine chain rupture as compared to analysis of bond lengths. Given two bonded carbon atoms C_i and $C_{j=i+1}$, we refer to the other atoms bonded to them as $C_{i-1}, H_{i,1}, H_{i,2}$ and $C_{j+1}, H_{j,1}, H_{j,2}$, respectively. We define $\alpha_{i,n=1,3}$ to be the angles $C_{i-1}\widehat{C_i}H_{i,1}$, $C_{i-1}\widehat{C_i}H_{i,2}$ and $H_{i,1}\widehat{C_i}H_{i,2}$, and $\beta_{j,n=1,3}$ to be $C_{j+1}\widehat{C_j}H_{j,1}$, $C_{j+1}\widehat{C_j}H_{j,2}$ and $H_{j,1}\widehat{C_j}H_{j,2}$, accordingly. $\sum_n \alpha_{i,n=1,3}$ and $\sum_n \beta_{j,n=1,3}$ equal 328.4° in perfectly tetrahedral (sp^3 hybridization) geometries, and 360° in planar (sp^2) molecules.

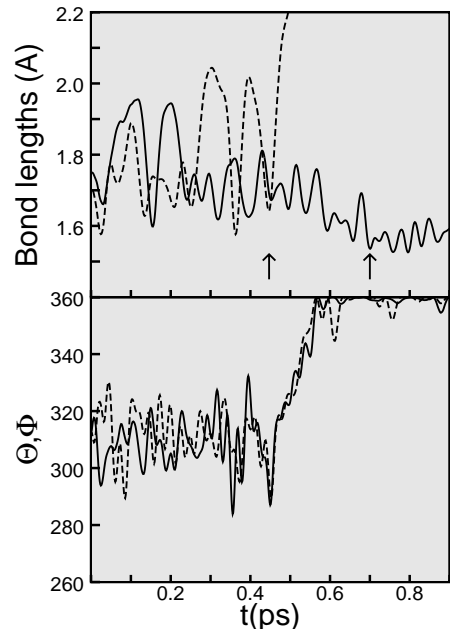


FIG. 10. Upper panel: time evolution of the lengths of the bonds located at the entrance and exit points of a trefoil knot with $N=28$ C atoms and end-to-end distance $L = 13.5 \text{ \AA}$. Lower panel: time evolution of the sums Φ and Θ of the bond angles about the atoms involved in the rupture (see text). Even when large bond-length deviations from equilibrium values occurred, the chemical bond did not break unless a change in the hybridization status of the key atoms was observed. Arrows indicate that the rupture and the readjustment of the system are separated by a time interval of about 250 fs .

When $L = 13.5 \text{ \AA}$, as shown in Fig. 9, the molecule finally snapped during the finite temperature run at the exit point of the knot with the two ends then strongly recoiling back. In the lower panel of Fig. 10 we report $\Phi_{22} = \sum_n \alpha_{22,n}$ and $\Theta_{23} = \sum_n \beta_{23,n}$ as functions of time. The fact that these quantities tended towards a value around 360° provides a simple, yet unequivocal, sign that the hybridization status of C_{22} and C_{23} atoms

had changed from sp^3 to sp^2 and, thus, that their chemical bond was broken. In the upper panel of the figure, we display the entrance and exit bond lengths for the same system. As previously discussed, very large deviations from the ground-state geometry are present for *both* bonds; however, only one of them finally ruptured. It is interesting to point out that, as marked by the arrows, the symmetric counterpart of the breaking bond needed about 250 fs to readjust and then oscillate around the equilibrium length of 1.54 Å. This is in agreement with our estimate of the typical time scale of an alkane of this size. An important quantity provided by first-principles MD is the electron charge density of the system, which is particularly useful in studies focused on the evolution of chemical bonds. In Fig. 11, a snapshot of the charge density after 0.8 ps of dynamical evolution is reported. Between the carbon atoms C_{22} and C_{23} there is a gap of charge density that confirms the bond breaking.

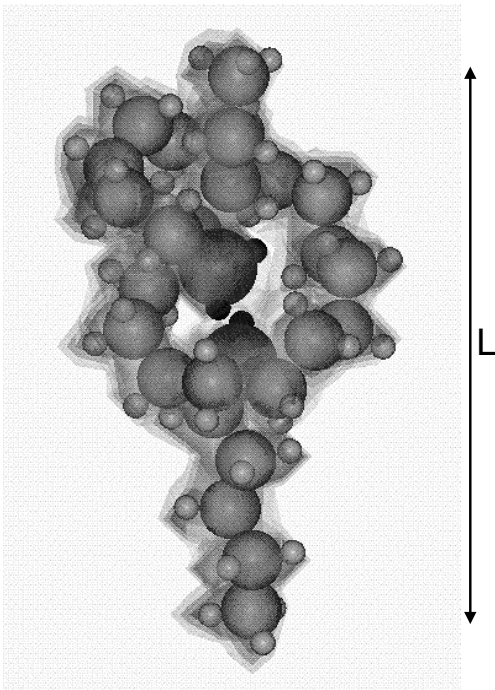


FIG. 11. Electronic charge density of the $C_{28}H_{58}$ trefoil at the breakpoint for $L = 13.5$ Å and $T = 300$ K. The two atoms involved in the bond breaking are drawn with a larger size and a darker color. A gap in the electronic density is clearly observable.

Other simulations performed using different initial conditions (*i.e.* heating rate, hydrogen atom optimization, etc.), or at larger tensile stress ($L = 13.75, 14.00$ Å) gave similar results; namely, bond breaking occurs randomly at one of the two symmetric entrance and exit points. In the latter case, when $L = 14.0$ Å, the molecule actually broke at *both* points; the amount of external load was so high that, after the first rupture, the system was not able to readjust quickly enough to avoid the second

break. This gave birth to three daughter radicals rather than two.

The amount of strain energy that a trefoil knot stores in a polyethylene chain before breaking is around 300 kcal/mol, and it has to contain at least 23 carbon atoms to be able to distribute such load along the molecule without breaking. This *ab initio* estimate is in agreement with results obtained via classical molecular dynamics [14]. The average load per bond in the tightest possible knot is ~ 13.3 kcal/mol, which is about 80% of the corresponding value in a linear alkane. This result, and the knot-induced location of the break along a chain, are in good agreement with known properties of macroscopic knots, which in turn suggests a universal behavior.

V. CONCLUSIONS

In conclusion, we have presented an atomic level description of the breaking of a polyethylene-like strand, both with and without a knot, when subjected to tensile loading. Specifically, we find that the mechanical strength and the strain distribution in a polymer just before breaking are profoundly influenced by the presence of a simple knot. Moreover, a knotted strand, unlike the unknotted one, does not break at the point where the tension is applied but, rather, at a point just outside the knot. Further, the presence of a knot weakens the rope in which it is tied. Our findings are in complete accord with the corresponding macroscopic phenomenon exhibited by a rope, which suggests that some of the other properties of knots known to sailors and fishermen for centuries [4] may well have a counterpart in the nanoscopic world of polymers.

This work has been supported in part by National Science Foundation. We thank E. Wasserman for focusing our attention on this problem, and M. Parrinello and J. Hutter for fruitful discussions. Special thanks go to H.S. Mei for help with graphics, and to K. Bagchi and D. Yarne for useful suggestions.

* To whom correspondence should be addressed. E-mail: saitta@cmm.chem.upenn.edu.

- [1] H.L. Frisch and E. Wasserman, *J. Am. Chem. Soc.* **83**, 3789 (1961).
- [2] G. Schill, *Catenanes, Rotaxanes, and Knots*, (Academic, New York, 1971).
- [3] D.M. Walba, *Tetrahedron* **41**, 3161 (1985).
- [4] C.W. Ashley, *The Ashley Book of Knots*, (Doubleday, New York, 1993).
- [5] P.-G. de Gennes, *Macromolecules* **17**, 703 (1984).
- [6] M.F. Atiyah, *The Geometry and Physics of Knots*, (Cambridge University Press, Cambridge, 1990).

- [7] S.A. Wasserman and N.R. Cozzarelli, *Science* **232**, 951 (1986); S.Y. Shaw and J.C. Wang, *Science* **260**, 533 (1993); T. Schlick and W.K. Olson, *Science* **257**, 1110 (1992).
- [8] M.D. Frank-Kamenetskii, A.V. Lukashin, and A.V. Volgodskii, *Nature* **258**, 398 (1975).
- [9] J.P.J. Michels and F.W. Wiegel, *Phys. Lett.* **90A**, 381 (1982).
- [10] E.J. van Rensburg, D.A.W. Summers, E. Wasserman, and S.G. Whittington, *J. Phys. A.* **25**, 6557 (1992).
- [11] R.K. Bayer, *Colloid Polym. Sci.* **272**, 910 (1994).
- [12] K. Iwata and M. Tanaka, *J. Phys. Chem.* **96**, 4100 (1992).
- [13] M.L. Mansfield, *Macromolecules* **27**, 5924 (1994).
- [14] M.L. Mansfield, *Macromolecules* **31**, 4030 (1998).
- [15] H.L. Frisch, *New J. Chem.* **17**, 697 (1993).
- [16] A.M. Saitta, P.D. Soper, E. Wasserman, and M.L. Klein, *Nature* **399**, 46 (1999).
- [17] N. Karasawa, S. Dasgupta, and W.A. Goddard III, *J. Phys. Chem.* **95**, 2260 (1991).
- [18] R. Car and M. Parrinello, *Phys. Rev. Lett.* **55**, 2471 (1985).
- [19] P. Giannozzi and S. Baroni, *J. Chem. Phys.* **100**, 8537 (1994); M. Bernasconi, M. Parrinello, G.L. Chiarotti, P. Focher, and E. Tosatti, *Phys. Rev. Lett.* **76**, 2081 (1996); M. Bernasconi, G.L. Chiarotti, P. Focher, M. Parrinello, and E. Tosatti, *Phys. Rev. Lett.* **78**, 2008 (1997); F. Ancilotto, G.L. Chiarotti, S. Scandolo, and E. Tosatti, *Science* **275**, 1288 (1997).
- [20] A.D. Becke, *Phys. Rev. A* **38**, 3098 (1988); C. Lee, W. Yang, and R.G. Parr, *Phys. Rev. B* **37**, 785 (1988).
- [21] N. Troullier and J.M. Martins, *Phys. Rev. B* **43**, 1993 (1991).
- [22] J.P. Perdew and Y. Wang, *Phys. Rev. B* **45**, 13244 (1992).
- [23] J.I. Siepmann, S. Karaborni, and B. Smit, *Nature* **365**, 330 (1993); C.J. Mundy, S. Balasubramanian, K. Bagchi, J.I. Siepmann, and M.L. Klein, *Faraday Discuss.* **104**, 17 (1996).
- [24] A. Borrmann, B. Montanari, and R.O. Jones, *J. Chem. Phys.* **106**, 8545 (1997); and references therein.
- [25] B. Montanari and R.O. Jones, *Chem. Phys. Lett.* **272**, 347 (1997); M.S. Miao, et al., *Phys. Rev. B* **54**, 10430 (1996); and references therein.